



Fracture penetration in planetary ice shells

Maxwell L. Rudolph*, Michael Manga

Department of Earth and Planetary Science, University of California, 307 McCone Hall, Berkeley, CA 94720-4767, USA

ARTICLE INFO

Article history:

Received 30 October 2007

Revised 18 September 2008

Accepted 5 October 2008

Available online 17 November 2008

Keywords:

Europa

Enceladus

Ices, mechanical properties

Satellites, surfaces

ABSTRACT

The proposed past eruption of liquid water on Europa and ongoing eruption of water vapor and ice on Enceladus have led to discussion about the feasibility of cracking a planetary ice shell. We use a boundary element method to model crack penetration in an ice shell subjected to tension and hydrostatic compression. We consider the presence of a region at the base of the ice shell in which the far-field extensional stresses vanish due to viscoelastic relaxation, impeding the penetration of fractures towards a subsurface ocean. The maximum extent of fracture penetration can be limited by hydrostatic pressure or by the presence of the unstressed basal layer, depending on its thickness. Our results indicate that Europa's ice shell is likely to be cracked under 1–3 MPa tension only if it is ≤ 2.5 km thick. Enceladus' ice shell may be completely cracked if it is capable of supporting ~ 1 –3 MPa tension and is less than 25 km thick.

© 2008 Elsevier Inc. All rights reserved.

1. Introduction

Liquid water may erupt on icy satellites of Saturn and Jupiter. The presence of topographic features on Europa such as smooth regions filling topographic lows and often bounded by ridges suggests that liquid water has erupted onto the ice-covered moon's surface (e.g., Fagents, 2003; Miyamoto et al., 2005; Prockter and Schenk, 2005). On Enceladus, a mixture of water vapor and ice is currently erupting from the "Tiger Stripe" fissures in the south polar region (Hansen et al., 2006). Although the requirement of liquid water is hotly debated (e.g., Kieffer and Jakosky, 2008), some models favor the eruption of liquid, rather than sublimation of a solid, on Enceladus (Porco et al., 2006). The ongoing eruption at Enceladus' South Pole appears to occur through tensile fractures (Hurford et al., 2007a).

Water confined to a subsurface ocean faces two mechanical impediments in reaching the surface. First, it is negatively buoyant with respect to ice and second, it needs a conduit through which to flow. If tensile stresses generated in an ice shell exceed the tensile strength of ice, a fracture will form and may provide the necessary conduit. Downward penetration of tensile fractures initiated at the surface is opposed by lithostatic pressure and by the absence of tensile stresses in the lower part of the shell, which become relaxed over long time scales (Nimmo, 2004; Manga and Wang, 2007). We use a numerical model to test the feasibility of fracturing an ice shell whose lower region does not support far-field tensile stresses.

Lee et al. (2005) and Qin et al. (2007) studied fracture penetration in an elastic medium with finite thickness and variable porosity. Their results indicate that the presence of a lower free-surface enables fractures to penetrate further than they would under otherwise identical conditions in a halfspace. Neither study accounts for the presence of a basal layer in which deviatoric stresses are relaxed, which is the focus of our study.

2. Background

Estimates of the thickness of Europa's ice shell lie within the range of about 1 km to at least 32 km (Billings and Kattenhorn, 2005). The maximum thickness of Europa's ice shell is constrained by the vertical extent of its ice + water shell, between 105 and 160 km depending on the composition and structure of the underlying rocky layers (Kuskov and Kronrod, 2005; Cammarano et al., 2006). Enceladus has a mean radius of 252.1 ± 0.2 km and may be partially- to fully-differentiated (Porco et al., 2006). In the latter case, the thickness of the ice + water shell is ~ 90 km, with an ice-only thickness of 10–90 km (Schubert et al., 2007).

In order to fracture an ice shell, there must be a physical mechanism capable of producing stresses in excess of the tensile strength of the material. Europa's shell is exposed to a diurnally varying tidal stress of magnitude 0.1 MPa (Hurford et al., 2007b). Nimmo (2004) calculated the stresses due to cooling and freezing at the base of an ice shell and found that extensional stresses exceed 10 MPa for shells that thicken to more than 10 km. When the compressibility of the underlying ocean is taken into account, stresses in the shell are reduced but still large, ~ 1 –3 MPa (Manga and Wang, 2007). The maximum stress due to non-synchronous rotation or true polar wander is of order 1–10 MPa (Leith and

* Corresponding author. Fax: +1 510 643 9980.

E-mail address: rudolph@berkeley.edu (M.L. Rudolph).

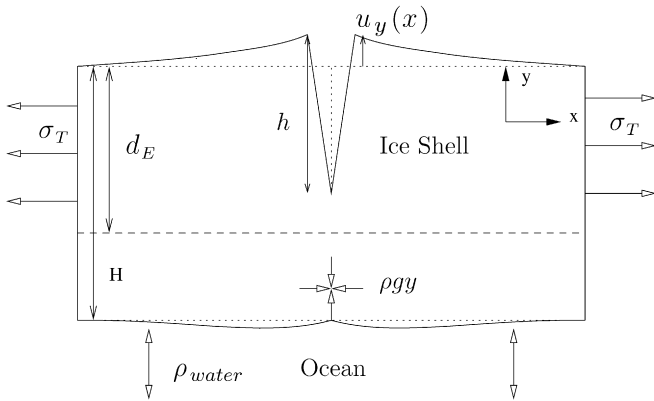


Fig. 1. Schematic illustration of our model geometry as described in Section 3.1. The dashed line at depth d_E represents the depth below which tensile stresses do not exist. The quantity $\Delta\rho$ is the difference in densities of water and ice, 90 kg m^{-3} .

McKinnon, 1996). Schenk et al. (2008) have suggested that surface features present on Europa indicate the occurrence of true polar wander. In combination, these stresses are sufficient to overcome the tensile strength of ice on Europa. Enceladus orbits Saturn with an eccentricity of 0.0047, producing tidal stresses on the order of 0.1 MPa (Hurford et al., 2007a). Nimmo and Pappalardo (2006) have proposed that Enceladus underwent diapir-induced re-orientation, which would produce tectonic stresses on the order of 10 MPa. Ocean pressurization due to ice shell thickening, should a subsurface ocean exist, could also produce stresses of 1–10 MPa for plausible changes in shell thickness (Manga and Wang, 2007).

3. Model

3.1. Physical model

We model the ice shell as a single homogeneous and isotropic linear elastic layer (Fig. 1). The entire shell deforms elastically on the time scale of crack propagation. Prior to fracturing, the upper region of the ice shell is stressed. Meanwhile, the lower, warmer part of the shell undergoes viscous deformation and tensile stresses will have relaxed. The depth at which viscous deformation dominates depends on the time scale over which stresses are applied. The upper boundary is a free-surface. The lower boundary does not support shear tractions and the normal component of stress must be continuous across this water–ice interface. The crack walls are prescribed to be free of shear tractions. Cracks are initiated at the upper surface because the applied tension is uniform across the elastic layer and hydrostatic pressure is zero at the surface. Once a fracture forms at the upper surface, the normal tractions exerted on its walls are the superposition of overburden and extensional stresses in the upper region of the ice shell, but only overburden stresses act in the lower, unstressed region. We assume that the acceleration due to gravity remains constant with depth, a reasonable assumption since the (highly uncertain) tensile strength of ice has a greater effect on our results.

In all cases, we let the Young's modulus $E = 5 \times 10^9 \text{ Pa}$ (Nimmo, 2004) and Poisson's ratio $\nu = 0.33$ (Schulson, 2001). A summary of the physical quantities used in our modeling is provided in Table 1.

The relevant thickness of the stressed upper layer depends on the time scale over which stresses are applied. The time scale governing viscous relaxation is the Maxwell time $\tau_M = \mu/E$. Nimmo (2004) assumed that viscous deformation dominates after $O(10)$ Maxwell times and defined the temperature at which the elastic-viscous transition occurs as $T = 180 \text{ K}$. This corresponds to an effective viscosity (assuming exponential dependence of viscosity on temperature) of $\sim 10^{18} \text{ Pa s}$ and a Maxwell time $\tau_M \approx 50$ years.

Table 1
Physical quantities used in the model.

	Europa	Enceladus
g	1.3 m s^{-2}	0.13 m s^{-2}
H	1–35 km	10–90 km
d_E/H	0.2–0.5	0.2–0.6
ρ_{ice}	910 kg m^{-3}	
σ_T	1–3 MPa	
E	5 GPa	
ν	0.33	

The temperature profile in an ice shell depends on whether or not the ice shell convects. Based on this choice of τ_M , if heat transfer occurs only through conduction, Europa's stressed layer has a fractional thickness (d_E/H) of about 0.5 and Enceladus' stressed layer comprises about 0.6 of its total ice shell thickness. Manga and Wang (2007) suggested time scales of $\tau_p = 10^5$ and 10^8 years for changes in stress due to ice shell thickening on Europa and Enceladus, respectively. By setting $10\tau_M = \tau_p$, we obtain corresponding temperatures of 140 K and 123 K and fractional stressed thicknesses of 0.2 for both satellites. We therefore primarily consider fractional stressed thicknesses of 0.2–0.5 for Europa and 0.2–0.6 for Enceladus.

In linear elastic fracture mechanics, the stress intensity factor describes the concentration of stresses at the tip of a crack (Irwin, 1957). There is a singularity in stress at the tip of a crack in a linear elastic material, which in nature is accommodated through plastic deformation. Here, we consider Mode-I fracture, in which crack walls undergo only normal displacement. A Mode-I fracture will grow if the crack-tip stress intensity factor, K_I , exceeds a critical value K_{IC} that is material-dependent. Stresses near a crack tip decay with $r^{-1/2}$ where r is distance from the crack tip, and K_I may be calculated by evaluating the normal traction acting on a crack-coplanar surface very close to the crack tip (Crouch and Starfield, 1983).

The tensile strength of ice on either satellite is the most poorly constrained physical property in our model. Fracture-free, avicicular ice Ih with a grain size of 1 mm has a measured tensile strength of 1.5 MPa at -10°C , while ice with finer grains may fail at 17 MPa (Schulson, 2001, 2006). Relevant temperatures on Europa and Enceladus are colder than those at which tensile strengths have been measured. Europa's low-latitude surface temperature is between 86 and 132 K (Spencer et al., 1999). The mean surface temperature on Enceladus is $75 \pm 3 \text{ K}$ and also varies with latitude (Grundy et al., 1999). The temperature increase across Europa's ice shell is about 170 K (Nimmo, 2004), resulting in laboratory-like conditions at the base of the shell. Both the compressive and tensile strengths of ice increase as temperature decreases, although the effect is less pronounced under tension (Schulson, 2001). Fractured or porous ice may be significantly weaker (e.g., Lee et al., 2005) and tensile strength may be scale-dependent; the in situ tensile strength of sea ice is $\sim 10^5 \text{ Pa}$ on length scales of hundreds of meters (e.g., Dempsey et al., 1999). We assume tensile strengths in the range of 1–3 MPa for consistency with previous studies (Manga and Wang, 2007; Leith and McKinnon, 1996).

3.2. Numerical method

We use an indirect boundary element method modified from the program TWODD (Crouch and Starfield, 1983) to calculate the displacements along fractures in a two dimensional linear elastic medium. Our first modification is the addition of a crack tip element that facilitates the calculation of stress intensity factors. We also account for gravity and buoyancy at the upper and lower boundaries. Rather than describing these forces as a body force

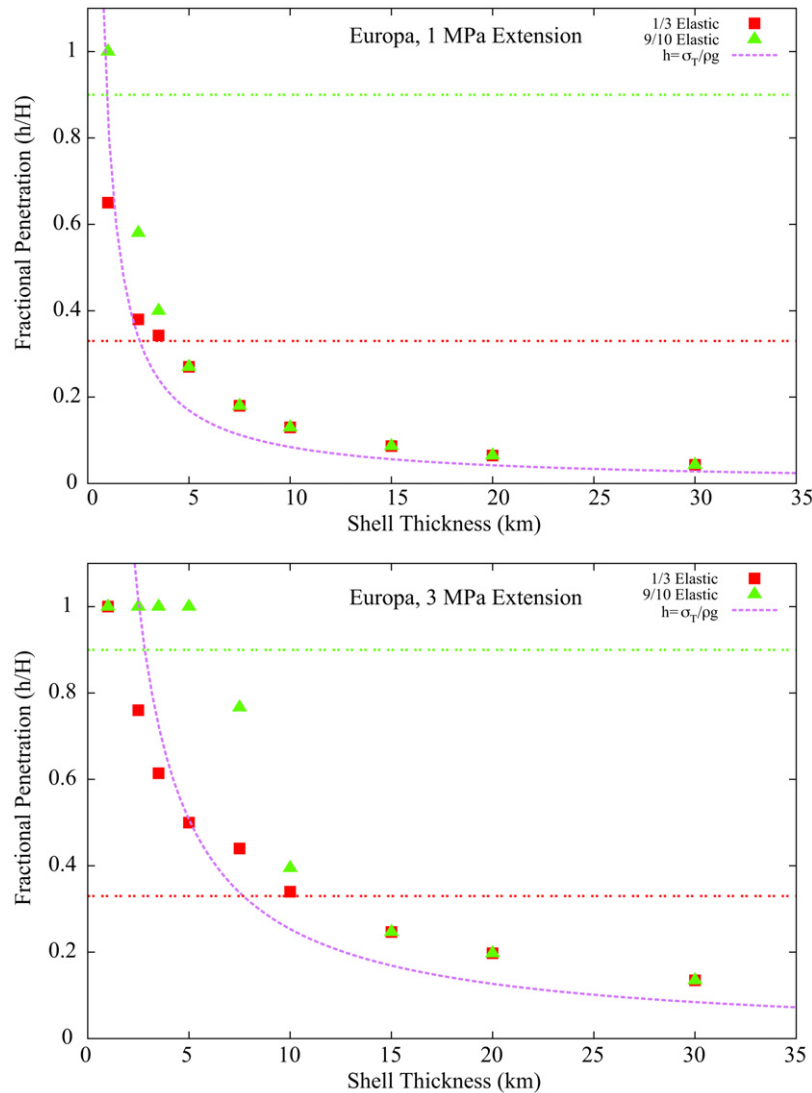


Fig. 2. Fractional penetration of fractures on Europa taking σ_T to be 1 MPa (top) and 3 MPa (bottom). The violet curve indicates the depth at which extension is balanced by hydrostatic compression in a completely-stressed halfspace.

acting throughout the shell, we approximate them by imposing normal tractions $t_y = \rho_i g u_y$ and $t_y = (\rho_w - \rho_i) g u_y$ on the upper and lower boundaries, respectively. Here, t_y is the (normal) boundary traction, u_y is vertical displacement, ρ is density, g is acceleration due to gravity, and the subscripts w and i denote water and ice. Because we treat the problem using linear elasticity and strains are small, this is a good approximation. Note that Fig. 1 reflects the boundary conditions described in Section 3.1 whereas in our numerical model, we have modified the boundary conditions to account for gravity. The upper and lower boundaries are both free of shear tractions. Each of these boundaries is prescribed to be 50 times greater in width than the shell thickness and element size varies linearly with distance from the crack, consistent with Qin et al. (2007). We begin each calculation by initiating a fracture with length l_0 at the upper boundary along the y -axis. The crack-tip stress intensity factor is computed by evaluating σ_{xx} a distance $r = 10^{-6} l_0$ from the crack tip (Crouch and Starfield, 1983). If the stress intensity factor is positive, we increase the length of the crack in 50 meter increments until K_I is no longer positive, consistent with the procedure used by Qin et al. (2007). Because the stress intensity factor decreases very rapidly near $K_I = 0$ as crack length increases in a hydrostatic stress field, this criterion for propagation produces the same results as using $K_I > K_{IC}$ to within

our 50-m crack length increment (Lee et al., 2007). By adopting this propagation criterion, the fractional penetrations that we obtain are upper bounds on what should be expected in a medium with nonzero fracture toughness.

Lachenbruch (1961) studied the propagation of cracks in an elastic halfspace subjected to the same horizontal loading conditions that we impose. Because his semi-analytic solution is not for the case of an elastic layer with a lower boundary, it does not adequately describe all of the cases that we analyzed. In order to validate our numerical model, we compared our predictions of fracture penetration depth to those predicted by the Lachenbruch solution. For the case $K_{IC} = 0$, we compared Lachenbruch's solution and our numerical solution for a typical crack on Enceladus where the stressed layer thickness $d_E = 6$ km and $\sigma_T = 3$ MPa. For consistency with the Lachenbruch solution, we removed the lower boundary from our model. The solution given by Lachenbruch (1961) for this case is $h = 0.36\sigma_T / (0.68\rho g)$. This solution yields $h = 13426$ m, whereas our numerical result is $h = 13400$ m. The two solutions agree to within our spatial resolution of 50 m. We also validated our code against analytic solutions for uniformly pressurized spherical cavities and cracks in infinite media (Crouch and Starfield, 1983).

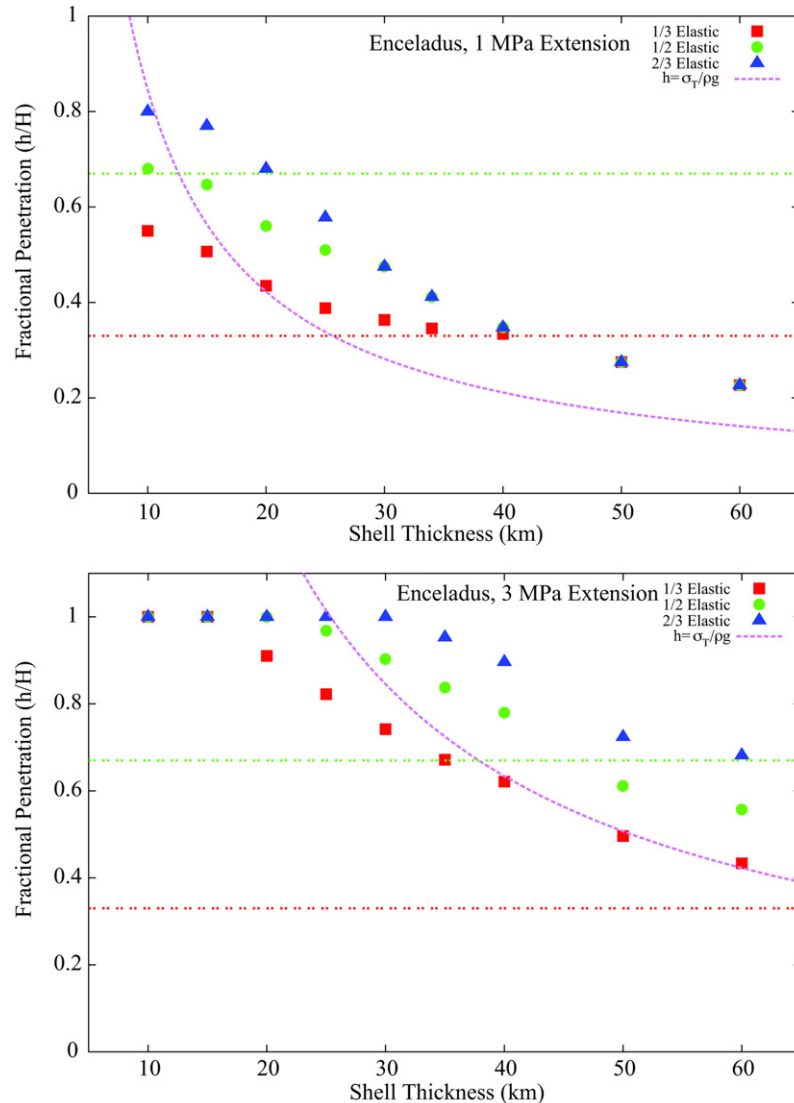


Fig. 3. Fractional penetration of fractures on Enceladus taking σ_T to be 1 MPa (top) and 3 MPa (bottom). The violet curve indicates the depth at which extension is balanced by hydrostatic compression in a completely-stressed halfspace.

4. Results and discussion

Figs. 2 and 3 show the fractional penetration depth (h/H) of cracks on Europa and Enceladus, respectively, as a function of tensile strength and stressed layer thickness. Throughout our analysis, we presume that the tensile strength is equal to the applied tensile stress in the upper layer. If the tensile strength is 1 MPa and the fractional thickness of Europa's stressed layer (d_E/H) is $1/3$, none of the shells that we considered can be completely cracked. If d_E/H is 0.9, European shells up to 5 km thick may be cracked under 3 MPa tension, but if the tensile strength of ice is 1 MPa, only very thin (≤ 1 km) shells may be cracked, despite this improbably large value of d_E/H . Fig. 4 (top) shows contours of minimum tensile stress necessary to completely fracture Europa's ice shell as a function of shell thickness and d_E/H . The shaded region in this figure illustrates the region of parameter space that we consider most reasonable. The thickest shell that may be completely cracked is about 2.5 km, consistent with only the smallest observationally-inferred thicknesses (Billings and Kattenhorn, 2005). Even if the tensile strength of ice is 10–20 MPa, about an order of magnitude greater than our preferred values, European ice shells thicker than about 9 km cannot be cracked (Fig. 4).

If the tensile strength of Enceladus' ice is 1 MPa, even a $2/3$ -stressed, 10-km shell (the thinnest shell we considered) cannot be cracked. If the tensile strength is 3 MPa, a $2/3$ -stressed 30 km shell may be cracked as may a $1/2$ -stressed 20 km shell. When the stressed layer comprises only $1/3$ of the total thickness, none of the model shells can be cracked. The shaded region in Fig. 4 (bottom) indicates our preferred range of parameters for which tensile fractures may completely penetrate Enceladus' shell. Given our assumed range for the tensile strength of ice and d_E/H between 0.2 and 0.6, ice shells up to 25 km in thickness may be completely cracked. Thus, it is possible that tensile fractures initiated at Enceladus' surface penetrate its ice shell and reach a subsurface ocean. If the low-temperature tensile strength of ice is an order of magnitude higher than we have assumed, the comparatively low gravitational acceleration on Enceladus will allow a large increase in crackable shell thickness; Shells up to and exceeding 60 km in thickness may be cracked under 10 MPa tension with d_E/H within our preferred range (Fig. 4).

The dashed violet curves in Figs. 2 and 3 indicate the depth at which hydrostatic compression negates the applied tension. Extension and hydrostatic compression balance at a depth $d_0 = \sigma_T / (\rho g)$. When $\sigma_T = 1$ MPa, $d_0 = 8.5$ km on Enceladus and $d_0 = 0.85$ km on

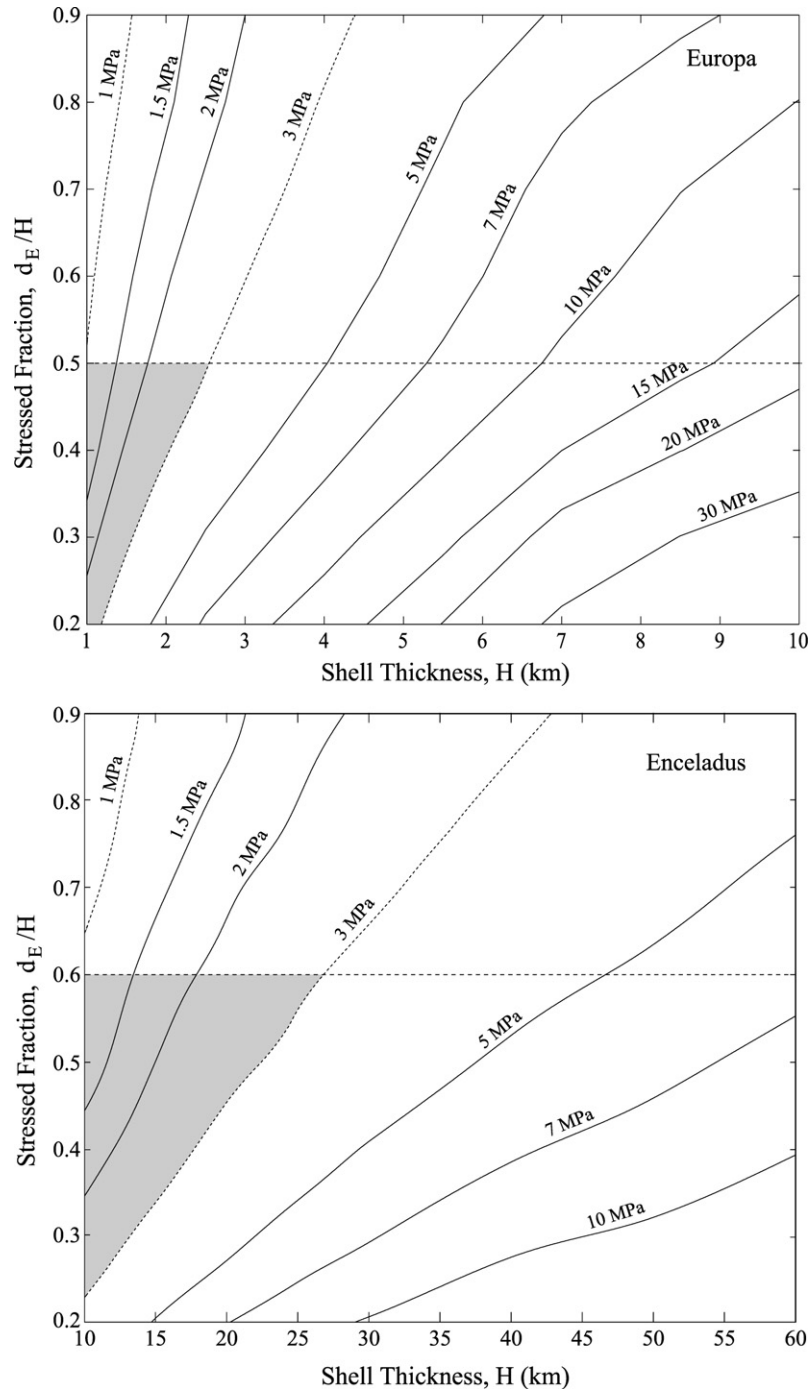


Fig. 4. Contour plots of σ_T necessary to completely fracture an ice shell on Europa (top) and Enceladus (bottom). Horizontal dashed lines indicate our preferred upper bounds on d_E/H . Dotted curves indicate contours of 1 and 3 MPa. The shaded regions represent the range of parameters using which shells may be completely cracked. These results are consistent with a modified form of the force balance used in Qin et al. (2007), which predicts that $d_E/H = (\rho g H)/(2\sigma_T)$ (W.R. Buck, private communication). Contours were generated using linear and spline interpolating functions on originally non-grid data.

Europa. In general, the fractures propagate past the depth at which horizontal stresses become compressive. Once a fracture has propagated past this depth, its tip is supported by stresses resulting from opening in the upper region (which experiences extensional stresses) and by the concentration of tensile stresses between the crack tip and the lower boundary. The latter effect is responsible for the large fractional penetrations seen clearly in Fig. 2 (bottom). This effect was also previously reported by Lee et al. (2005). If the stressed thickness is smaller than d_0 , crack penetration is limited by the extent of the stressed layer. When the stressed layer extends below d_0 , crack penetration is limited solely by hydrostatic

compressive stress. The former limiting scenario applies to thin shells and counteracts the stress concentration due to the presence of a lower boundary. Lee et al. (2005) predicted that thin European shells could be easily cracked under tension but neglected the effect of the unstressed lower region on crack penetration.

As in Manga and Wang (2007), we assume that the ice shell is unfractured and is capable of supporting tensile stresses of up to the tensile strength over the characteristic time scale of stress increase. We have also assumed that tensile strength does not vary significantly with depth. The effect of temperature on tensile strength within the ice shell may be negligible (Schulson, 2001),

but porosity may substantially reduce tensile strength in the upper region of the shell (Lee et al., 2005). In this case, the upper shell would be easily fractured (possibly by the diurnal tidal stress), while the lower shell could only be cracked by the larger stresses due to ice shell thickening (Manga and Wang, 2007), non-synchronous rotation (e.g., Leith and McKinnon, 1996), or polar wander (e.g., Ojakangas and Stevenson, 1989).

5. Conclusion

It is unlikely that tensile fractures initiated at Europa's surface can propagate all the way to a subsurface ocean unless its ice shell is less than 2.5 km thick. When the tensile strength of ice is taken as 3 MPa, no shell whose thickness is greater than ~5 km may be fractured. If the unstressed part of the ice shell is 2/3 the total thickness, only a ≤ 1 km shell may be fractured. Because gravitational acceleration is an order of magnitude smaller on Enceladus than on Europa, it is much more likely that Enceladus' ice shell may be cracked, and if cracking occurs, water is more likely to erupt (Manga and Wang, 2007). Considerably larger fractional penetrations may be achieved if tensile cracks on either satellite can become filled with fluid (e.g., Crawford and Stevenson, 1988), which is beyond the scope of this paper.

Acknowledgments

Stephen Crouch provided helpful correspondence regarding the displacement discontinuity method. Edwin Kite and Eric Gaidos provided useful comments and discussion. We thank Roger Buck and John Dempsey for helpful reviews that enhanced the clarity of our manuscript. This work has been supported in part by NASA grants NNX08AL26G and NNA04CC02A.

References

- Billings, S.E., Kattenhorn, S.A., 2005. The great thickness debate: Ice shell thickness models for Europa and comparisons with estimates based on flexure at ridges. *Icarus* 177, 397–412.
- Cammarano, F., Lekic, V., Manga, M., Panning, M., Romanowicz, B., 2006. Long-period seismology on Europa. 1. Physically consistent interior models. *J. Geophys. Res. (Planets)* 111, E12009.
- Crawford, G.D., Stevenson, D.J., 1988. Gas-driven water volcanism in the resurfacing of Europa. *Icarus* 73, 66–79.
- Crouch, S., Starfield, A., 1983. *Boundary Element Methods in Solid Mechanics*. George Allen & Unwin, London.
- Dempsey, J.P., Adamson, R.M., Mulmule, S.V., 1999. Scale effects on the in-situ tensile strength and fracture of ice. Part II. First-year sea ice at Resolute, N.W.T. *Int. J. Fracture* 95 (1), 347–366.
- Fagents, S.A., 2003. Considerations for effusive cryovolcanism on Europa: The post-Galileo perspective. *J. Geophys. Res.* 108 (E12), doi:10.1029/2003JE002128. 5139.
- Grundy, W.M., Buie, M.W., Stansberry, J.A., Spencer, J.R., Schmitt, B., 1999. Near-infrared spectra of icy outer Solar System surfaces: Remote determination of H₂O ice temperatures. *Icarus* 142, 536–549.
- Hansen, C.J., Esposito, L., Stewart, A.I.F., Colwell, J., Hendrix, A., Pryor, W., Shemansky, D., West, R., 2006. Enceladus' water vapor plume. *Science* 311, 1422–1425.
- Hurford, T.A., Helfenstein, P., Hoppa, G.V., Greenberg, R., Bills, B.G., 2007a. Eruptions arising from tidally controlled periodic openings of rifts on Enceladus. *Nature* 447, 292–294.
- Hurford, T.A., Sarid, A.R., Greenberg, R., 2007b. Cycloidal cracks on Europa: Improved modeling and non-synchronous rotation implications. *Icarus* 186, 218–233.
- Irwin, G., 1957. Analysis of stresses and strains near the end of a crack traversing a plate. *J. Appl. Mech.* 24 (4), 361–364.
- Kieffer, S.W., Jakosky, B.M., 2008. Planetary science: Enceladus—Oasis or ice ball? *Science* 320 (5882), 1432–1433.
- Kuskov, O.L., Kronrod, V.A., 2005. Internal structure of Europa and Callisto. *Icarus* 177, 550–569.
- Lachenbruch, A., 1961. Depth and spacing of tension cracks. *J. Geophys. Res.* 66 (12), 4273–4292.
- Lee, S., Pappalardo, R.T., Makris, N.C., 2005. Mechanics of tidally driven fractures in Europa's ice shell. *Icarus* 177, 367–379.
- Lee, S., Pappalardo, R.T., Makris, N.C., 2007. Reply to "Comment on Mechanics of tidally driven fractures in Europa's ice shell". *Icarus* 189, 598–599.
- Leith, A.C., McKinnon, W.B., 1996. Is there evidence for polar wander on Europa? *Icarus* 120, 387–398.
- Manga, M., Wang, C.-Y., 2007. Pressurized oceans and the eruption of liquid water on Europa and Enceladus. *Geophys. Res. Lett.* 34, L07202.
- Miyamoto, H., Mitri, G., Showman, A.P., Dohm, J.M., 2005. Putative ice flows on Europa: Geometric patterns and relation to topography collectively constrain material properties and effusion rates. *Icarus* 177, 413–424.
- Nimmo, F., 2004. Stresses generated in cooling viscoelastic ice shells: Application to Europa. *J. Geophys. Res. (Planets)* 109, E12001.
- Nimmo, F., Pappalardo, R.T., 2006. Diapir-induced reorientation of Saturn's moon Enceladus. *Nature* 441, 614–616.
- Ojakangas, G.W., Stevenson, D.J., 1989. Polar wander of an ice shell on Europa. *Icarus* 81, 242–270.
- Porco, C.C., Helfenstein, P., Thomas, P.C., Ingersoll, A.P., Wisdom, J., West, R., Neukum, G., Denk, T., Wagner, R., Roatsch, T., Kieffer, S., Turtle, E., McEwen, A., Johnson, T.V., Rathbun, J., Veverka, J., Wilson, D., Perry, J., Spitale, J., Brahic, A., Burns, J.A., DelGenio, A.D., Dones, L., Murray, C.D., Squyres, S., 2006. Cassini observes the active south pole of Enceladus. *Science* 311, 1393–1401.
- Prockter, L., Schenk, P., 2005. Origin and evolution of Castalia Macula, an anomalous young depression on Europa. *Icarus* 177, 305–326.
- Qin, R., Buck, W.R., Germanovich, L., 2007. Comment on "Mechanics of tidally driven fractures in Europa's ice shell" by S. Lee, R.T. Pappalardo, and N.C. Makris [2005. *Icarus* 177, 367–379]. *Icarus* 189, 595–597.
- Schenk, P., Matsuyama, I., Nimmo, F., 2008. True polar wander on Europa from global-scale small-circle depressions. *Nature* 453, 368–371.
- Schubert, G., Anderson, J.D., Travis, B.J., Palguta, J., 2007. Enceladus: Present internal structure and differentiation by early and long-term radiogenic heating. *Icarus* 188, 345–355.
- Schulson, E.M., 2001. Brittle failure of ice. *Eng. Fracture Mech.* 68 (17–18), 1839–1887.
- Schulson, E.M., 2006. The fracture of water ice Ih: A short overview. *Meteorit. Planet. Sci.* 41, 1497–1508.
- Spencer, J.R., Tamppari, L.K., Martin, T.Z., Travis, L.D., 1999. Temperatures on Europa from Galileo PPR: Nighttime thermal anomalies. *Science* 284, 1514–1516.